

# *Numerical Study on Performance of Packed Bed Latent Heat Storage Integrated with Solar Water Heating System*

Wang Xianglei<sup>1,a,\*</sup>, Shi Yanfang<sup>2,b,\*</sup>, Wang Kun<sup>1,c,\*</sup>, Li Bin<sup>1,d,\*</sup>, Li Yu<sup>1,e,\*</sup>, Zhu Xiaomei<sup>1,f,\*</sup>,  
Wang Yunfei<sup>1,g,\*</sup>

<sup>1</sup>Department of Chemical Engineering, Ordos Institute of Technology, Ordos, China

<sup>2</sup>Yijinhuluo Campus of Ordos No.1 High School, Ordos, China

<sup>a</sup>wxl19830403@aliyun.com, <sup>b</sup>372199673@qq.com, <sup>c</sup>wangkun.105@163.com, <sup>d</sup>904431341@qq.com,  
<sup>e</sup>274143275@qq.com, <sup>f</sup>eo zhuxm@163.com, <sup>g</sup>276333481@qq.com

\*Corresponding author

**Keywords:** Packed bed latent heat storage, local thermal nonequilibrium, nonisothermal flow multiphysics, heat storage time, porous media

**Abstract:** Thermal energy storage (TES) units are used to accumulate thermal energy from solar, geothermal, or waste heat sources. The thermal capacity of these tanks can be further increased by including latent heat, which gives rise to latent heat storage (LHS) units. Typically, LHS tanks contain spherical capsules filled with paraffin as phase change material. This study deals with the numerical evaluation of thermal performance of a packed bed latent heat TES unit integrated with solar flat plate collector. The apparent heat capacity formulation provides an implicit capturing of the phase change interface, by solving for both phases a single heat transfer equation with effective material properties. Local thermal nonequilibrium approach is considered in packed LHS units. The nonisothermal flow multiphysics feature is added to model containing a free and porous media flow and heat transfer in porous media. Paraffin solid wax phase fraction and temperature evolutions are studied. This paper reveals influence of inlet velocity, solar collector power, melting temperature interval, latent heat of fusion, thermal conductivity amplification factor. The time required for heat storage completion is negatively correlated with inlet velocity, solar collector power and thermal conductivity amplification factor. The time required for heat storage completion is positively correlated with latent heat of fusion. The time required for heat storage completion is independent of melting temperature interval.

## 1. Introduction

The utilization of the renewable energy resources has attracted many efforts in recent years due to the continuous increase in the level of greenhouse gas emissions [1]. Its implementation has some challenges such as a gap between demand and supply because of the fluctuating nature [2]. Thermal energy storage is a crucial solution to fill this gap and help to produce power steadily by solar energy [3, 4].

Sensible heat storage and latent heat storage (LHS) are the basic types of thermal energy storage

techniques. LHS technique provides a high energy storage density and has the capacity to store heat as latent heat of fusion at a constant temperature. Materials used for latent heat thermal energy storage are known as phase change materials (PCMs) and may undergo solid-solid, solid-liquid and liquid-gas phase transformations [5]. PCMs require their upper and lower phase transition temperatures to be within the operational temperature range for a given application [6]. Due to abundance of solar energy and time required for charging process, it is important to study discharge process in order to better utilize the energy stored with regards to time and amount of energy needed for each application.

The PCM-based heat storage in the packed bed is one of the most suitable storage units [7]. A packed bed is a volume of porous media obtained by packing particles of selected material such as spherical capsules filled with PCM into a container [8].

Ismail and Stuginsky [9] presented comparative numerical investigation on packed bed thermal models suitable for sensible and latent heat thermal storage systems. Ismail and Henriq uez [10] presented a numerical model to simulate a storage system composed of spherical capsules filled with PCM and packed inside a cylindrical tank. They studied the influence of the geometrical and operational parameters of the system on the charging and discharging processes. Various phase change materials such as AlSi12 [11], paraffin wax [12], meristic acid [13] and molten-salt [14] have been used in the study of packed bed thermal storage.

According to the previous literature, different numerical models have been developed to analyze the performance of the thermal energy storage systems. These models can be mainly divided into single phase models, Schumann's model, concentric dispersion model, and continuous solid phase model [15].

In this paper, it models the flow through a packed-bed storage tank, and it includes the effects of heat transfer with phase change and local thermal nonequilibrium while charging the LHS unit. Warm water flows through the tank, and during thermal charging it is continuously heated up by a solar collector that delivers a power. The temperature difference at the tank's inlet and outlet is given by the relations of the power and the flow rate. The influences of power and flow rate will be investigated.

## 2. Model description

### 2.1. Physical geometry and material properties

The model geometry is shown in Figure 1. Geometry, material properties, and operating conditions are taken from [16]. The thermo-physical properties of paraffin are listed in Table 1.

Table 1: Thermo-physical properties of paraffin.

Material Property	Paraffin, solid	Paraffin, liquid
Melting temperature, $T_m$ (°C)	60	
Latent heat of fusion, $L$ (J/Kg)	213	
Density, $\rho$ (kg/m <sup>3</sup> )	861	778
Heat capacity, $C_p$ (J/kg/K)	1850	2384
Thermal conductivity, $k$ (W/m/K)	0.4	0.15

Due to considerable amount of calculations, required time and memory in the 3-D form of the present study; an axisymmetric 2-D model has been chosen. Paraffin-filled spherical capsules with a diameter of  $d_p=55\text{mm}$  are stored in a tank of 36 cm in diameter and 47 cm in height. The porosity of this bed is  $\varepsilon_p=0.49$ . The temperature is initially set to 32°C. Warm water flows through the tank with a flow rate of  $V_{in}=2\text{L/min}$ , and during thermal charging it is continuously heated up by a solar

collector that delivers a power of  $Q_u=375$  W. The temperature difference at the tank's inlet and outlet is given by the relation.

$$\frac{Q_u}{V_{in}} = \rho C_p (T_{in} - T_{out}) \quad (1)$$

## 2.2. Free and porous media flow

The velocity field is calculated by solving Eqs. (2) and (3) as below

$$\rho \nabla \cdot u = 0 \quad (2)$$

$$\frac{1}{\varepsilon_p} \rho (u \cdot \nabla) u \frac{1}{\varepsilon_p} = \nabla \cdot [-pI + K] - (\mu \kappa^{-1} + \beta \rho |u| + \frac{Q_m}{\varepsilon_p^2}) u + F \quad (3)$$

Ergun equation describes the flow through the packed bed, which estimates the pressure drop as a function of the velocity field  $u$

$$\nabla p = -\frac{\mu}{\kappa} - \frac{1.75(1-\varepsilon_p)}{d_p \varepsilon_p^3} \rho |u| u \quad (4)$$

Here,  $\mu$  (Pa·s) and  $\rho$  (kg/m<sup>3</sup>) are the viscosity and density of water,  $d_p$  (m) is the spheres' diameter, and  $\varepsilon_p$  the porosity. The permeability  $\kappa$  (m<sup>2</sup>) of the packed bed is given by

$$\kappa = \frac{d_p^2 \varepsilon_p^3}{150(1-\varepsilon_p)^2} \quad (5)$$

### 2.2.1. Boundary condition

Inlet: warm water flows through the tank with a flow rate of  $V_{in}=2$ L/min.

## 2.3. Heat transfer in porous media

Heat transfer in fluid takes place by convection and it is calculated by solving energy Eq. (6) as follows:

$$\rho_f C_{p,f} \frac{\partial T_f}{\partial t} + \rho_f C_{p,f} u_f \cdot \nabla T_f + \nabla \cdot q_f = Q_f \quad (6)$$

The energy Eq. (7) is solved in order to calculate heat transfer in solid, which takes place by conduction mechanism, as below:

$$\rho_s C_{p,s} \frac{\partial T_s}{\partial t} + \nabla \cdot q_s = Q_s \quad (7)$$

### 2.3.1. Local thermal nonequilibrium

The relative large diameter of the capsules as compared to the tank dimensions suggests a significant temperature difference between the encapsulated paraffin and the surrounding water flow, thus a local thermal nonequilibrium (LTNE) approach is considered in this study.

The heat transferred from the paraffin-filled capsules to the water is modeled with a heat source.

$$Q_f = \frac{q_{sf}}{\varepsilon_p} (T_s - T_f) \quad (8)$$

Here,  $T_s$  and  $T_f$  are the paraffin and water temperatures, and  $q_{sf}$  (W/m<sup>3</sup>/K) is the interstitial convective heat transfer coefficient, which for spherical capsules reads

$$q_{sf} = \frac{6(1 - \varepsilon_p)}{d_p} h_{sf} \quad (9)$$

The interstitial heat transfer coefficient  $h_{sf}$  follows a Nusselt number correlation. Convection inside the capsules is neglected, thus paraffin is treated as a solid or immobile liquid.

$$h_{sf} = \left[ d_p \left( \frac{1}{k_f Nu} + \frac{1}{10k_s} \right) \right]^{-1} \quad (10)$$

### 2.3.2. Phase change heat transfer

Temperature distribution in PCMs is calculated by solving Eq. (7). In this interval, the material phase is modeled by a smoothed function,  $\theta(\theta_1, \theta_2)$ , representing the fraction of phase before transition. This method considers that the phase change occurs in the interval of  $(T_m - \Delta T_m/2)$  and  $(T_m + \Delta T_m/2)$ . Until the temperature is less than  $(T_m - \Delta T_m/2)$  the value of function of phase change,  $\theta_2$ , is zero and when the temperature exceeds  $(T_m + \Delta T_m/2)$ , its value is 1. During the phase transition process, the density is the average density of the solid and liquid. During the phase change, heat conductivity, heat capacity are also changed. Eqs. (11)-(12) represent these changes, where the indices 1 (solid) and 2 (fluid) indicate a material in phase 1 or in phase 2, respectively.:

$$k_s = \theta_1 k_1 + \theta_2 k_2 \quad (11)$$

$$C_{p,s} = \theta_1 C_{p,1} + \theta_2 C_{p,2} + L_{1 \rightarrow 2} \frac{\partial \alpha_m}{\partial T} \quad (12)$$

$$\theta_1 + \theta_2 = 1 \quad (13)$$

The mass fraction of fluid paraffin,  $\alpha_m$ , is defined from  $\theta_1$  and  $\theta_2$  according to:

$$\alpha_m = \frac{1}{2} \frac{\theta_2 - \theta_1}{\theta_1 + \theta_2} \quad (14)$$

### 2.3.3. Boundary condition

Inflow: the inlet temperature varies and is given by the relation solar collector power and flow rate.

### 2.3.4. Stop condition

When the minimum temperature of porous medium exceeds 70 °C, calculation stops.



Figure 1: Schematics of the packed bed filled with paraffin spherical capsules. And top cut point (0, 0.42), center (0, 0.235) and low point (0, 0.05) are shown in the Figure.

## 2.4. Nonisothermal flow

The nonisothermal flow multiphysics feature can be added to a model containing a single-phase flow and a heat transfer interface, to realize the two-way coupling between the two interfaces.

## 3. Results and discussion

### 3.1. Temperature evolutions

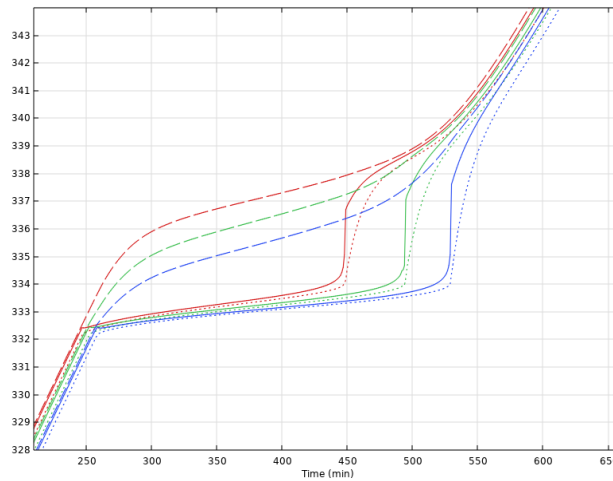


Figure 2: Evolution of water (dashed), paraffin (dotted) and average porous medium temperature (solid) during phase change for top cut point (red), center cut point (green) and low cut point (blue) position.

Figure 2 shows the evolution of the paraffin temperature, the water temperature, and the weighted average (porous-medium) temperature. During the phase change, the encapsulated paraffin is not in thermal equilibrium with the surrounding water. The top cut point temperature is higher than the center and low cut point. Measuring the water temperature at the inlet or the outlet

does not give accurate information about neither the temperature inside the capsules nor the phase in which the paraffin wax is.

### 3.2. Paraffin solid wax phase fraction vs paraffin wax temperature

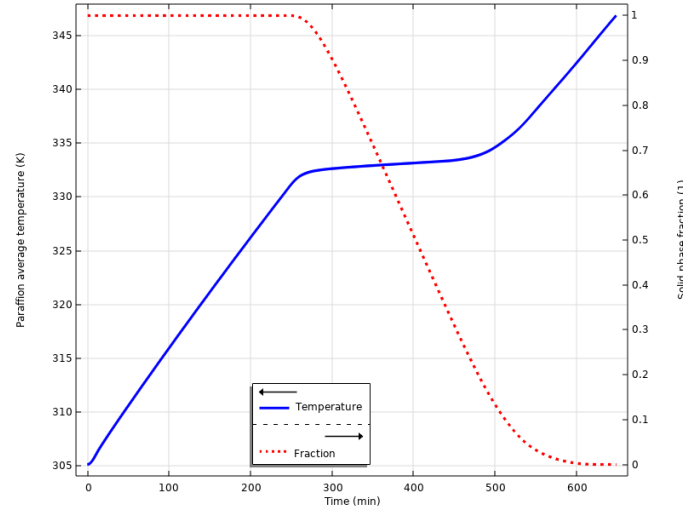


Figure 3: Evolution of paraffin average temperature vs paraffin solid phase fraction.

Figure 3 shows the evolution of the paraffin average temperature vs paraffin average solid fraction. Melting temperature of paraffin is 333.15K, during phase change process, paraffin average temperature changes relatively slowly, but paraffin average solid phase fraction changes relatively rapidly. During non-phase change process, paraffin average temperature changes relatively rapidly, but paraffin average solid phase fraction almost doesn't change.

### 3.3. Influence of inlet velocity

Effect of the HTF inlet velocity on the thermal performance of the packed bed is investigated in this section. The latent heat storage tank is considered fully charged as soon as a temperature of 70°C is reached everywhere. As shown in Figure 4, the time required for heat storage completion decreases with increasing flow rate. But the decreasing speed of completion time is getting smaller and smaller until it reaches a constant value. And the convection heat flux has little effect on the heat storage process.

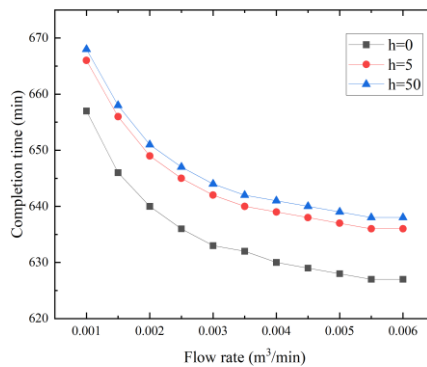


Figure 4: The relationship between heat storage completion time and flow rate under different convection heat fluxes ( $h$  (W/m²/K)).

### 3.4. Influence of solar collector power

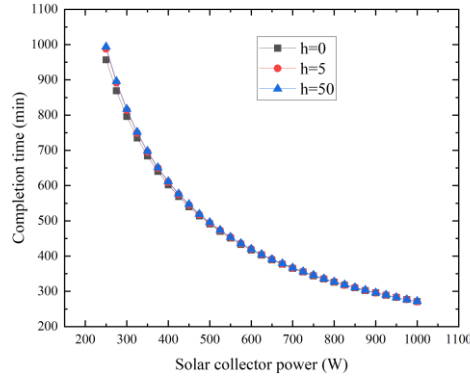


Figure 5: The relationship between heat storage completion time and solar collector power under different convection heat fluxes ( $h$  ( $\text{W}/\text{m}^2/\text{K}$ )).

Figure 5 shows the relationship between heat storage completion time and solar collector power. The time required for heat storage completion decreases with increasing solar collector power. But the decreasing speed of completion time is getting smaller and smaller. And the convection heat flux has little effect on the heat storage process. When solar collector power is high enough, the convection heat flux has no effect on the heat storage process.

### 3.5. Influence of melting temperature interval

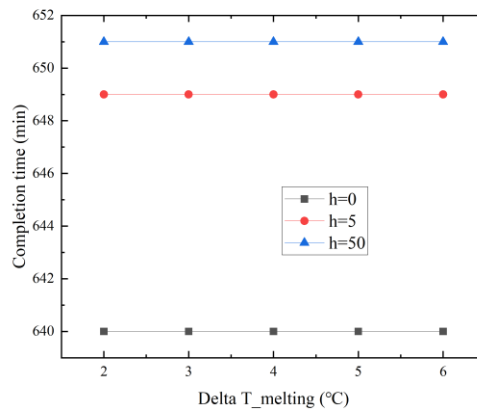


Figure 6: The relationship between heat storage completion time and melting temperature interval under different convection heat fluxes ( $h$  ( $\text{W}/\text{m}^2/\text{K}$ )).

As shown in Figure 6, the melting temperature interval has no effect on the heat storage process due to zero increase in heat exchange and heat transfer speed.

### 3.6. Influence of latent heat of fusion

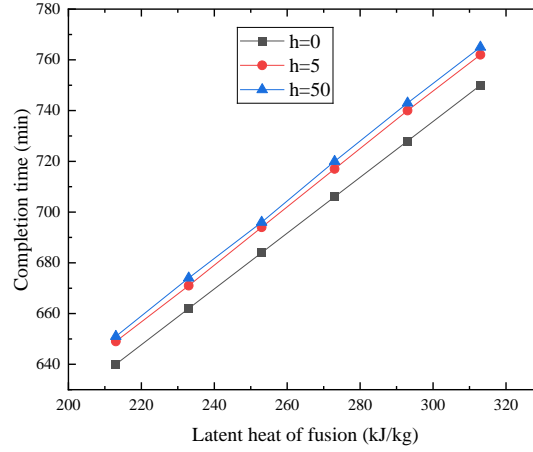


Figure 7: The relationship between heat storage completion time and latent heat of fusion under different convection heat fluxes ( $h$  ( $\text{W}/\text{m}^2/\text{K}$ )).

Figure 7 shows that the time required for heat storage completion increases linearly with increasing latent heat of fusion due to increase in heat storage capacity. And latent heat of fusion has effects on the heat storage process especially on the high latent heat of fusion condition.

### 3.7. Influence of thermal conductivity amplification factor

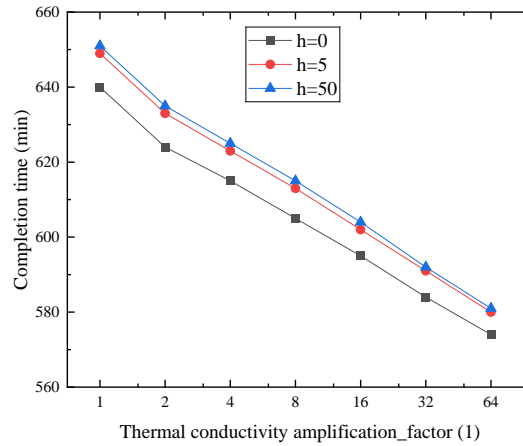


Figure 8: The relationship between heat storage completion time and thermal conductivity amplification factor under different convection heat fluxes ( $h$  ( $\text{W}/\text{m}^2/\text{K}$ )).

It can be seen from figure 8, the time required for heat storage completion increases almost linearly with decreasing thermal conductivity amplification factor's logarithm due to increase in heat transfer speed.



## 4. Conclusions

A CFD model was developed to investigate the discharge process of a packed bed of latent storage system integrated with solar flat plate collector. The apparent heat capacity is used to describe the heat capacity and latent heat. Local thermal nonequilibrium approach is considered in packed LHS units. The nonisothermal flow multiphysics feature is added to model containing a free and porous media flow and heat transfer in porous media. During the phase change, the encapsulated paraffin is not in thermal equilibrium with the surrounding water. The time required for heat storage completion is negatively correlated with inlet velocity, solar collector power and thermal conductivity amplification factor. The time required for heat storage completion is positively correlated with latent heat of fusion. The time required for heat storage completion is independent of melting temperature interval.

## Acknowledgements

The authors acknowledge the financial support provided by Natural Science Foundation of Inner Mongolia Autonomous Region of China (No. 2023LHMS05033, No.2022MS02004), National Natural Science Foundation of China (No. 51666002) and Ordos Doctoral Funding Program.

## References

- [1] M. Kenisarin, K. Mahkamov. Solar energy storage using phase change materials [J]. *Renewable and Sustainable Energy Reviews*, 2007, 11:1913–1965.
- [2] I. Dincer, C. Acar. A review on clean energy solutions for better sustainability [J]. *International Journal of Energy Research*, 2015, 39 (5): 585–606.
- [3] T. Kousksou, P. Bruel, A. Jamil, T. El Rhafiki, Y. Zeraoui. Energy storage: applications and challenges [J]. *Solar Energy Materials and Solar Cells*, 2014, 120: 59–80 VolsPart A.
- [4] T.U. Daim, X. Li, J. Kim, S. Simms. Evaluation of energy storage technologies for integration with renewable electricity: quantifying expert opinions [J]. *Environmental Innovation and Societal Transitions*, 2012, 3: 29–49.
- [5] S. Hasnain, (1998) Review on sustainable thermal energy storage technologies, part I: heat storage materials and techniques [J]. *Energy Conversion and Management*, 1998, 39 (11):1127–1138.
- [6] K. Pielichowska, K. Pielichowski. Phase change materials for thermal energy storage [J].*Progress in Materials Science*, 2014, 65: 67–123.
- [7] H. Mehling, L.F. Cabeza. *Heat and Cold Storage with PCM* [R]. Springer, 2008.
- [8] H. Singh, R.P. Saini, J.S. Saini. A review on packed bed solar energy storage systems [J]. *Renewable and Sustainable Energy Reviews*, 2010, 14: 1059–1069.
- [9] K.A.R. Ismail, R. Stuginsky Jr. A parametric study on possible fixed bed models for pcm and sensible heat storage [J]. *Applied Thermal Engineering*, 1999, 19: 757–788.
- [10] K.A.R. Ismail, J.R. Henriq uez. Numerical and experimental study of spherical capsules packed bed latent heat storage system [J]. *Applied Thermal Engineering*, 2002, 22: 1705–1716.
- [11] L. Geissbühler, M. Kolman, G. Zanganeh, A. Haselbacher, A. Steinfeld. Analysis of industrial-scale high-temperature combined sensible/latent thermal energy storage [J].*Applied Thermal Engineering*, 2016, 101: 657–668.
- [12] A. Felix Regin, S.C. Solanki, J.S. Saini. An analysis of a packed bed latent heat thermal energy storage system using PCM capsules: numerical investigation [J]. *Renewable Energy*, 2009, 34: 1765–1773.
- [13] S. Wu, G. Fang. Dynamic performances of solar heat storage system with packed bed using myristic acid as phase change material [J]. *Energy Build*, 2011, 43:1091–1096.
- [14] M. Wu, C. Xu, Y.-L. He. Dynamic thermal performance analysis of a molten-salt packed-bed thermal energy storage system using PCM capsules [J]. *Applied Energy*, 2014, 121:184–195.
- [15] G. Alvaro de, F. Luisa, Cabeza. Numerical simulation of a PCM packed bed system: a review [J]. *Renewable and Sustainable Energy Reviews*, 2017, 69:1055–1063.
- [16] N. Nallusamy, S. Sampath, R. Velraj. Study on performance of a packed bed latent heat thermal energy storage unit integrated with solar water heating system[J]. *Journal of Zhejiang University-SCIENCE A*, 2006, 7:1422–1430.